

OBSERVATIONS OF THE GAS RESERVOIR AROUND A STAR FORMING GALAXY IN THE EARLY UNIVERSE

BRENDA L. FRYE¹, DAVID V. BOWEN², MAIREAD HURLEY¹, TODD M. TRIPP³, XIAOHUI FAN⁴, BRADLEY HOLDEN⁵, PURAGRA GUHATHAKURTA⁵, DAN COE⁶, TOM BROADHURST⁷, EIICHI EGAMI⁴, G. MEYLAN⁸

Draft version July 10, 2021

ABSTRACT

We present a high signal-to-noise spectrum of a bright galaxy at $z = 4.9$ in 14 h of integration on VLT FORS2. This galaxy is extremely bright, $i_{850} = 23.10 \pm 0.01$, and is strongly-lensed by the foreground massive galaxy cluster Abell 1689 ($z = 0.18$). Stellar continuum is seen longward of the Ly α emission line at $\sim 7100 \text{ \AA}$, while intergalactic H I produces strong absorption shortward of Ly α . Two transmission spikes at $\sim 6800 \text{ \AA}$ and $\sim 7040 \text{ \AA}$ are also visible, along with other structures at shorter wavelengths. Although fainter than a QSO, the absence of a strong central ultraviolet flux source in this star forming galaxy enables a measurement of the H I flux transmission in the intergalactic medium (IGM) in the vicinity of a high redshift object. We find that the effective H I optical depth of the IGM is remarkably high within a large 14 Mpc (physical) region surrounding the galaxy compared to that seen towards QSOs at similar redshifts. Evidently, this high-redshift galaxy is located in a region of space where the amount of H I is much larger than that seen at similar epochs in the diffuse IGM. We argue that observations of high-redshift galaxies like this one provide unique insights on the nascent stages of baryonic large-scale structures that evolve into the filamentary cosmic web of galaxies and clusters of galaxies observed in the present universe.

Subject headings: galaxies: clusters: general — galaxies: clusters: individual (A1689)—galaxies: high-redshift—gravitational lensing—techniques: spectroscopic—methods: data analysis

1. INTRODUCTION

Hydrodynamic simulations tell us that dark matter near the epoch of galaxy formation collapses into an ordered filamentary pattern, the so-called “cosmic web.” In turn, this cosmic web is thought to cradle high-redshift galaxies in dense nodes that are opaque to the extragalactic ultraviolet background radiation. Observations of H I surrounding these high-redshift objects provide information on the likely reservoirs from which galaxies assemble their gas. Hitherto, it has only been possible to measure H I opacities towards bright Quasi-stellar Objects (QSOs); unfortunately, the high ultraviolet flux from the QSOs ionizes the hydrogen clouds in their vicinity, thereby making the determination of H I cloud physical conditions unreliable close to the QSO.

New techniques and facilities in the past decade have enabled detailed observational studies of the IGM in the early universe ($z > 5$). For example, the spectra of high-redshift QSOs show a plethora of H I Ly α absorption lines, the “Ly α forest”, as well as lines from a wide va-

riety of heavier elements, all of which provide detailed information about the high-redshift IGM along the line-of-sight towards the QSO. Around the QSOs themselves, however, the ultraviolet flux is so high that it typically ionizes the surrounding gas. Thus QSOs are not ideal for studying the pervasive IGM close to the QSO. Instead, we suggest that bright galaxies may provide better probes for the study of IGM conditions in the proximity of high-redshift objects, as these objects emit fewer ultraviolet photons than QSOs do.

The subject of this paper is the Ly α forest in the spectrum of an unusually bright high-redshift galaxy at $z = 4.866$ (Frye et al. 2002, 2007). The galaxy is situated behind the massive galaxy cluster Abell 1689 ($z = 0.183$), which magnifies the starlight of this background object by a factor of 10.3 by the effect of gravitational lensing (Broadhurst et al. 2005). Multicolor Hubble Space Telescope (HST) imaging of one of the faint lensed images, hereafter designated A1689.7.1, is shown in Figure 1. We assume a cosmology for this paper of $H_0 = 70 \text{ km s}^{-1} \text{ Mpc}^{-1}$, $\Omega_{m,0} = 0.3$, and $\Omega_{\Lambda,0} = 0.7$.

2. OBSERVATIONS AND SPECTRUM

Our spectrum of A1689.7.1 is made possible with present telescopes only by the combination of strong lensing *and* unusually-long observations. We obtained the spectrum for A1689.7.1 in 14 hours at the Very Large Telescope (VLT) with the Focal Reducer and low-dispersion Spectrograph (FORS2) in 2001 June and July and report a spectral resolution of $R = \lambda/\Delta\lambda \approx 530^9$. We fluxed the data with the standard star LTT9239, and

⁹ The observations were made on VLT/Kueyen FORS2 under observing programme 67.A-0618B

¹ School of Physical Sciences, Dublin City University, Glasnevin, Dublin 9, Ireland

² Department of Astrophysical Sciences, Peyton Hall, Princeton University, Princeton, NJ 08540

³ Department of Astronomy, University of Massachusetts, Amherst, MA 01003

⁴ Department of Astronomy and Steward Observatory, University of Arizona, Tucson, AZ 85721

⁵ UCO/Lick Observatory, University of California, Santa Cruz, CA 95064

⁶ Jet Propulsion Laboratory, M/S 169-327, 4800 Oak Grove Drive, Pasadena, CA 91109

⁷ School of Physics and Astronomy, Tel Aviv University, Ramat Aviv 69988, Israel

⁸ Laboratoire d’Astrophysique, Ecole Polytechnique Fédérale de Lausanne (EPFL) Observatoire, CH-1290, Sauverny, Suisse

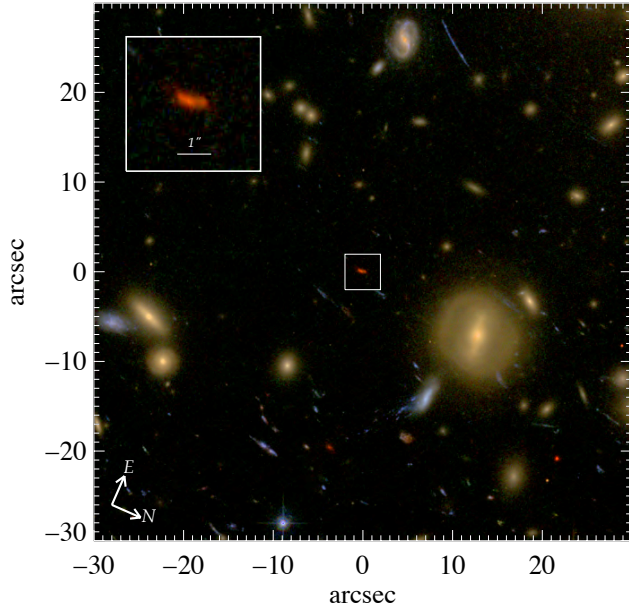


FIG. 1.— HST Advanced Camera for Surveys (ACS) *gri* optical photo of A1689.7.1 and surrounding region near the center of the galaxy cluster Abell 1689 ($z = 0.18$). A single galaxy at $z = 4.9$ has been gravitationally-lensed by this foreground galaxy cluster (with member galaxies visible here as yellow spheroid-shaped objects) into a system of three arclets; A1689.7.1 is the brightest of the three and is shown above and in the inset. This arclet is extremely bright, $i_{775} = 23.10 \pm 0.01$ magnitudes, after being magnified by a factor of 10.3. A1689.7.1 is also spatially resolved, with an estimated unlensed angular size of $0.094''$, corresponding to an intrinsic linear size of only 600 pc. A1689.7.1 was discovered as a part of a ground-based galaxy redshift survey (Frye et al. 2002, 2007).

performed the reductions with a code written by the first author in IDL designed to maximize the signal to noise of background-limited objects. See ? for more details on this purpose-built spectroscopic reduction package.

The spectrum of A1689.7.1 (Figure 2) shows an H I Ly α emission line and several strong low- and high-ionization metal absorption lines detected against the stellar continuum. On the basis of a mean velocity difference of $v = 470 \text{ km s}^{-1}$ between the positional centroids of the metal absorption features and the Ly α emission line, we apply an offset correction (Adelberger et al. 2003) and measure a systemic redshift of $z = 4.866$ for the galaxy. Interestingly, Ly α absorption immediately shortward of the emission line is not obviously damped at our spectral resolution, with a column density of $\log [N_{HI} (\text{cm}^{-2})] < 20.0 \pm 0.3$ dex (see Figure 2 inset). At our spectral resolution, the detected absorption lines are strongly-saturated and thus are not suitable for deriving metallicities. The most unusual feature of the spectrum is the broad absorption trough in the Ly α forest first appearing at the Ly α emission feature and extending towards shorter wavelengths. Although two transmission spikes are visible at $\sim 6800 \text{ \AA}$ and $\sim 7040 \text{ \AA}$, nearly 100% of the continuum is absorbed between wavelengths of 6850 - 7100 \AA .

What might this absorption represent? It is likely that we are detecting the presence of many more overlapping Ly α forest clouds closer to the galaxy than can survive the UV radiation field of QSOs at comparable distances. At the resolution of our data, individual Ly α forest lines

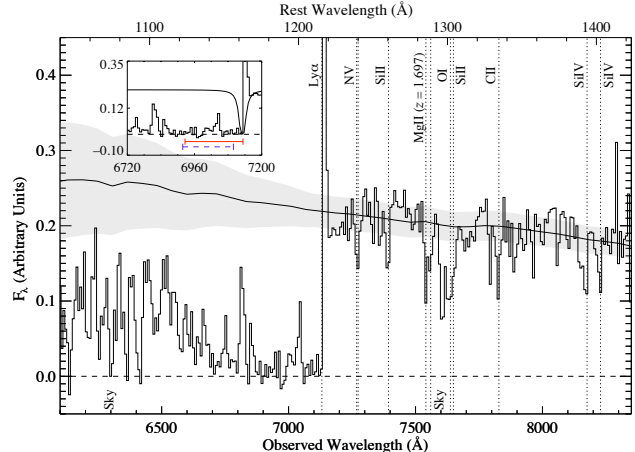


FIG. 2.— VLT FORS2 spectrum of A1689.7.1 at $z = 4.866$. The stellar continuum of the galaxy is seen longward of the Ly α emission line at $\sim 7100 \text{ \AA}$, while intergalactic H I produces strong absorption shortward of Ly α . Two transmission spikes at $\sim 6800 \text{ \AA}$ and $\sim 7040 \text{ \AA}$ are also visible, along with other structures at shorter wavelengths. The data enable a measurement of the flux transmission along the line of sight to this star-forming galaxy. The best-fit Bruzual & Charlot (2003) model spectrum without corrections for dust extinction and attenuation by the intervening Ly α forest is overlaid, including a gray region marking our 1σ continuum-placement uncertainties. We select a Chabrier initial mass function (Padova 1994), stellar evolution tracks, and solar metallicity for the model, and give the details regarding the fitting procedure in §4. The inset figure shows a theoretical H I Ly α profile absorption fit to the data, with horizontal bars delimiting the physical extents of the proximity zone for a QSO (red solid line), and the extent of the first of the five equally-spaced redshift bins in our study over which we measure the H I opacity (blue-dashed line), respectively. Owing to the lack of a significant proximity zone for our galaxy, a new physical scale is probed close to a high redshift object within a ~ 14 physical Mpc radius (blue dashed line).

cannot be resolved, and we would see only the effects of a large number of blended lines. It is also possible that the enhanced absorption could be from only a few overlapping, but very high- N_{HI} clouds, but we might then expect to see more metal absorption lines from these clouds redward of the Ly α emission line, which are absent in our data. Even less likely is that this H I overdensity signals the late completion of cosmic reionization, as recent observational studies have set convincing constraints for this epoch at $z \gtrsim 6.3$ (Fan et al. 2006; Songaila 2004).

We explore the nature of this remarkably large absorption trough with a comparison to the Ly α absorption seen towards their brighter counterpart objects, the QSOs. QSOs produce radiation fields that ionize hydrogen over large, ~ 16 physical Mpc regions at $z = 5$ (Fan et al. 2006) (red solid line in Figure 2 inset). Although evidence has emerged of a softening of this proximity effect in the transverse direction on small scales of $\lesssim 1.5$ Mpc from studies of QSO pairs (Bowen et al. 20006; Tytler et al. 2007). detailed studies of the Lyman-series forest are made routinely only outside the ionizing influence of the QSOs. In contrast, ordinary star forming galaxies have modest proximity zones of size $0.1h^{-1}$ physical Mpc (Adelberger et al. 2003), thereby enabling the study of H I and its structure in the vicinity of deep potential wells where the gas is not ionized. Despite the advantage of a small proximity zone, galaxies suffer from being much fainter in the ultraviolet. Unlike the vast majority of star-forming galaxies, our target is bright because it is

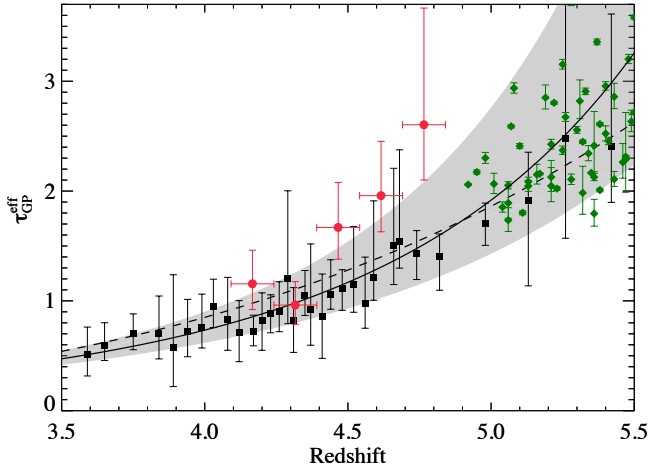


FIG. 3.— H I overdensities in the high redshift universe. The Gunn-Peterson effective optical depth, τ_{GP}^{eff} , is measured in the Ly α forest of the spectrum for A1689.7.1. The values for τ_{GP}^{eff} in five redshift bins of $\Delta z = 0.15$ each in the rest frame of the source (red points), are compared to measurements towards QSOs [square-shaped points (Songaila 2004) and diamond-shaped points (Fan et al. 2006)]. While τ_{GP}^{eff} is expected to lie close to the bulk of the QSO points and model predictions [dashed curve (Fan et al. 2006) and solid curve (Becker et al. 2007)], surprisingly, there is an excess in τ_{GP}^{eff} along the line of sight to A1689.7.1 at $z > 4.5$. The highest redshift point is the most deviant; it corresponds to a physical region of size 14 (physical) Mpc and this suggests that there is more H I gas close to the galaxy compared to the standard IGM. The error bars in the data are dominated by the intrinsic scatter of the continuum flux levels due to the stochastic nature of the absorption in the IGM, or sample variance, and also include continuum-placement uncertainties and shot noise.

strongly-lensed, thereby yielding a spectrum suitable for measuring the transmitted flux T in the Ly α forest in the proximity of a *galaxy*.

3. H I FLUX TRANSMISSION

We calculate the Gunn-Peterson (GP) optical depth (Gunn & Peterson 1965), $\tau_{GP}^{eff} = -\ln(T)$, where T is the ratio of the average observed flux to the average unabsorbed continuum flux, $T = \langle f_{\lambda}/f_{cont} \rangle$, and f_{cont} is determined by stellar synthesis models fit to the photometric data. We compute τ_{GP}^{eff} in several redshift bins extending from a wavelength clear of the red wing of Ly β up to the blue edge of our model fit to the H I in the source (blue dashed line in Figure 2 inset delimits the extent of the highest redshift bin). Uncertainties in τ_{GP}^{eff} are dominated by the intrinsic scatter of the continuum flux levels due to the stochastic nature of the absorption in the IGM, or sample variance (Tepper-García & Fritze 2008), but also include continuum placement errors and shot noise. Figure 3 shows the results measured from the A1689.7.1 spectrum and compares our values for τ_{GP}^{eff} to those observed toward a large sample of QSOs (Fan et al. 2006; Songaila 2004).

We emphasize that the values for τ_{GP}^{eff} are measured in the same way towards both the QSOs and the galaxy, and after first excluding the proximity zone, thereby yielding information only on the pervasive IGM; that is the IGM immediately *outside* the photoionizing influence of the source. Assuming τ_{GP}^{eff} to be the same in the standard IGM towards *any* background object, we would expect

τ_{GP}^{eff} to rise steadily towards A1689.7.1 with absorption redshift following the bulk of the QSO points. Compared to the predictions of a power-law model based on the density distribution (Fan et al. 2006) and a lognormal optical depth distribution (Becker et al. 2007), τ_{GP}^{eff} measurements toward A1689.7.1 are in good agreement at $z < 4.5$; at $z > 4.5$, however, we see a significant excess in τ_{GP}^{eff} . If the underlying mass distribution were unaltered by the presence of the galaxy, then this highest-redshift point, the one in closest physical proximity of the galaxy, should have also followed the behavior of the other points. The highest redshift point is the most deviant; it corresponds to a physical radius ~ 14 (physical) Mpc, and this result suggests that there is more H I gas close to the galaxy compared to the standard IGM.

4. POPULATION SYNTHESIS MODELING

A1689.7.1 is imaged in several bands, as follows: $i_{775} = 23.10 \pm 0.01$ (HST ACS), $J_{110} = 23.10 \pm 0.02$ (HST NICMOS), $H = 23.45 \pm 0.38$ and $K_s = 23.45 \pm 0.35$ (Son of Isaac Instrument on ESO New Technology Telescope), and $P_{3.6} = 23.3 \pm 0.02$, and $P_{4.5} = 23.34 \pm 0.03$ (IRAC on Spitzer Space Telescope). The observing details for these data are discussed elsewhere (Frye et al. 2007). From these data we set initial constraints on the galaxy age and dust extinction. Our high quality J_{110} , $P_{3.6}$ and $P_{4.5}$ points indicate only a modest H I Balmer series continuum break at rest-frame $\sim 4000 \text{ \AA}$ and thus a young underlying stellar population dominated by O stars with a minimum age of $t \gtrsim 10$ Myr (Figure 4). The age of the universe for our adopted cosmology sets the upper limit on the galaxy age of 1.2 Gyr. The dust extinction, as parameterized by the color excess $E(B - V)$, is fit with a broad range spectral energy distribution templates. From these fits it is found that any model with $E(B - V) > 0.1$ provides a poor fit to the slope of data, as the continuum becomes significantly flatter in the blue with the addition of even moderate amounts of dust. Thus we restrict our parameter space to $E(B - V) \leq 0.1$.

Model spectral energy distributions are generated using the stellar synthesis code of Bruzual & Charlot (2003). We select a Chabrier initial mass function (Padova 1994), stellar evolution tracks, and solar metallicity. We choose a single starburst model with a range of decay rates τ and a star formation rate (SFR) that depends exponentially on τ as follows: $SFR(t) \propto \exp(t/\tau)$ with $\tau = 0.1, 0.2, 0.3, 0.5, 1, \text{ and } 1.2$ Gyr. Continuous star-formation models are also considered, as approximated by selecting τ to be the age of the universe at $z = 5$, and we do not consider more complicated star formation histories. For each τ , three parameters remain to be fit to the data: age t , $E(B - V)$, and stellar mass M_* . A suite of models are constructed over the allowable parameter space for these three variables, and each model is corrected for the effects of dust extinction (Calzetti et al. 2000), and attenuation by the intervening Lyman-series forest (Madau 1995).

We compute synthetic photometry on our models by a convolution of the model spectra with the observed filter bandpass transmission functions. We compare the synthetic photometry with the observed photometric values until the lowest value of reduced χ^2 is obtained. Figure 4 shows our best fit model to the joint variation of the parameters of dust extinction, age, and mass, with

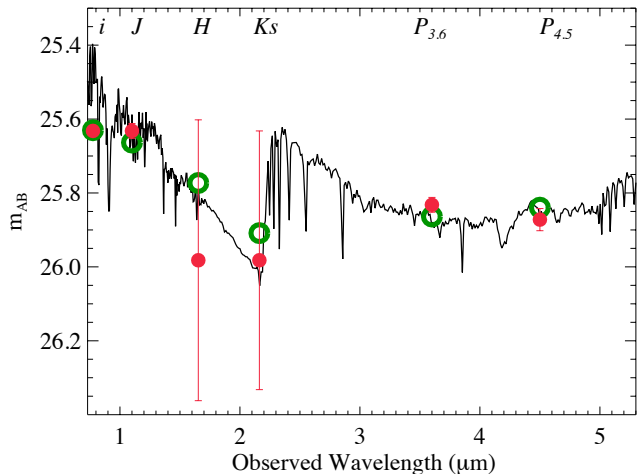


FIG. 4.— The best-fit spectral energy distribution for our galaxy, with dust extinction and attenuation by the IGM. The red solid circles indicate the values for our observed photometry in the various filter bandpasses, as marked. We construct a suite of models and perform synthetic photometry on the models (green open circles) until a model is found for which the reduced χ^2_r statistic is minimized with respect to the observed photometry. Our best-fit model is for a young, low-mass and dust-free galaxy.

values: $E(B - V) = 0.0^{+0.02}_{-0.00}$, $t = 100^{+14}_{-14}$ Myr, and $M^* = 7.3 \pm 0.70 \times 10^8 M_\odot$. Note that as the exponentially-decaying models are normalized to have a total mass of $1M_\odot$ as $t \rightarrow \infty$, we obtain the mass for A1689.7.1 by the flux normalization that yields the lowest value for the reduced χ^2 fit. Our best fit is for a no-dust model. We compute formal χ^2 uncertainties that represent 68 % uncertainties for our input model. We follow the prescription in Cash (1976) originally developed for use with X-ray spectral data that allows for the joint estimation of confidence intervals.

The best fit synthetic spectrum is also shown in Figure 2 in the main text, but *without* corrections for dust extinction and absorption by the intervening Ly α forest. This intrinsic form is used to define the unabsorbed continuum level f_{cont} for A1689.7.1 against which the flux transmission of the Ly α forest is measured.

5. DISCUSSION

Despite the strong magnification, the intrinsic luminosity of the galaxy is not high; we measure an unabsorbed luminosity of $L_{1400} = 7.7 \times 10^{28}$ ergs s $^{-1}$ Hz $^{-1}$, and an unlensed $K = 24.5$, two magnitudes fainter than K^* at $z = 3$ (Shapley et al. 2001). Galaxies at $z \gtrsim 5$ are faint, and hence only a few high quality spectra exist (Price et al. 2007; Kawai et al. 2006; Dow-Hygelund et al. 2007; Franx et al. 1997). Some of these are at $z > 6$ where τ_{GP}^{eff} is expected to be high (from the QSO measurements), but the spectrum of the gamma-ray burst GRB060510B at $z = 4.94$ (Price et al. 2007). shows some similar characteristics to the spectrum of A1689.7.1. The IGM transmission measured over a broad redshift bin of the former is $T = 0.18$, similar to the values observed toward QSOs. However, this broad average smears out the structure in τ_{GP}^{eff} as a function of redshift. The GRB060510B

spectrum shows evidence of higher than expected GP optical depth extending beyond the region affected by the damped Ly α absorption at the redshift of the GRB host. It would be interesting to reanalyze this GRB spectrum using smaller redshift bins. H I opacities were also measured inside the proximity zones of QSOs; although significantly ionized, the proximity zones are found to have neutral hydrogen fractions that exceed theoretical expectations. This indicates that at least some QSOs are also found in regions of gaseous overdensity with large sizes of $15h^{-1}$ Mpc (Guimarães et al. 2007).

Might A1689.7.1 still be in the process of accreting much of its mass from its overdense surrounding cosmic structure? Theoretical models predict that H I gas is funneled into young galaxies via large-scale filamentary structures (Kereš et al. 2005; Birnboim & Dekel 2003). We have presented here observational evidence that H I column densities are higher than expected near one high-redshift galaxy. Based on the large physical size implied by the H I excess, it is unlikely that this gas will accrete onto a single galaxy. Alternatively, post-starburst galaxies are known to drive high-velocity outflows with velocities of $\lesssim 2000$ km s $^{-1}$ in low-ionization stages such as Mg II (Tremonti et al. 2007). Given sufficient time, the observed excess of H I optical depth could be explained by such an outflow; however A1689.7.1 is too young by a significant factor given the best fit stellar age of 100 ± 14 Myr. On the other hand, QSOs are known to drive outflows with terminal velocities in excess of 10^4 km s $^{-1}$. A1689.7.1 does not show obvious signatures of being an AGN, but even if there was a low-metallicity outflow undetected in our spectrum, the velocities would still fall short by more than a factor of ten of that required to explain the H I excess. As more data become available to study the neutral H I absorption towards the several recently discovered strongly-lensed LBGs, it may be found to be typical for high-redshift objects, both galaxies and QSOs, to be located in regions of space with neutral hydrogen gas fractions significantly larger than that of the pervasive IGM. This re-evaluation of the H I structure in the densest regions of the universe at these epochs will provide the necessary calibration for modeling the formation and evolution of galaxies in the early universe.

This work is based on data from the HST ACS instrument, which was developed under NASA contract NAS5-32865, and on the Very Large Telescope FORS2 instrument. B. L. F. is supported by Science Foundation Ireland Research Frontiers Programme Grant PHY008. D. V. B. is funded through NASA Long-Term Space Astrophysics grant NNG05GE26G. The work of D. A. C. was carried out at Jet Propulsion Laboratory, California Institute of Technology, under a contract with NASA. We thank Holland Ford, Garth Illingworth, Avi Loeb, Rogier Windhorst, and Sergey Cherkis for discussions, and Rychard Bouwens for the HST NICMOS *J*-band photometry.

Facilities: HST(ACS), VLT.

REFERENCES

- Adelberger, K. L., Steidel, C. C., Shapley, A. E., & Pettini, M. 2003, ApJ, 584, 45
- Becker, G. D., Rauch, M., & Sargent, W. L. W. 2007, ApJ, 662, 72

- Birnboim, Y., & Dekel, A. 2003, MNRAS, 345, 349
- Bowen, D., et al. 2006, ApJ, 645, L105
- Broadhurst, T., et al. 2005, ApJ, 621, 53
- Bruzual, G., & Charlot, S. 2003, MNRAS, 344, 1000
- Calzetti, D., Armus, L., Bohlin, R. C., Kinney, A. L., Koornneef, J., & Storchi-Bergmann, T. 2000, ApJ, 533, 682
- Cash, W. 1976, A&A, 52, 307
- Dow-Hygelund, C., et al. 2007, ApJ, 660, 47
- Fan, et al. 2006, AJ, 132, 117
- Franx, M., Illingworth, G. D., Kelson, D. D., van Dokkum, P. G., & Tran, K.-V. 1997, ApJ, 486, L75
- Frye, B., Broadhurst, T., & Benítez, N. 2002, ApJ, 568, 558
- Frye, B., et al. 2007, ApJ, 665, 921
- Guimarães, R., Petitjean, P., Rollinde, E., de Carvalho, R. R., Djorgovski, S. G., Srianand, R., Aghaee, A., & Castro, S. 2007, MNRAS, 377, 657
- Gunn, J. E., & Peterson, B. A. 1965, ApJ, 142, 1633
- Kawai, K., et al. 2006, Nature, 440, 184
- Kereš, D., Katz, N., Weinberg, D. H., & Davé, R. 2005, MNRAS, 363, 2
- Madau, P. 1995, ApJ, 441, 18
- Price, et al. 2007, ApJ, 663, L57
- Shapley, A. E., Steidel, C. C., Adelberger, K. L., Dickinson, M., Giavalisco, M., & Pettini, M. 2001, ApJ, 562, 95
- Songaila, A. 2004, AJ, 127, 2598
- Tepper-García, T., & Fritze, U. 2008, MNRAS, 383, 1671
- Tremonti, C. A., Moustakas, J., & Diamond-Stanic, A. M. 2007, ApJ, 663, L77
- Tytler, D., et al. 2007, ArXiv e-prints, 0711.2308